The View from the Top:
CALIOP Ice Water Content in the Uppermost Layer of Tropical Cyclones

Melody A. Avery[1]; Min Deng[2]; Anne Garnier[3]; Andrew Heymsfield[4]; Jacques Pelon[5]; Kathleen A. Powell[1]; Charles R. Trepte[1]; Mark A. Vaughan[1]; David M. Winker[1]; Stuart Young[6]

[1]*NASA Langley Research Center, Hampton, VA, USA*, [2]*University of Wyoming, Laramie, WY, USA*, [3]*Science Systems and Applications, Inc., Hampton, VA, USA*, [4]*National Center for Atmospheric Research, Boulder, CO, USA*, [5]*LATMOS, UPMC-UVSQ-CNRS, Paris, France*, [6]*CSIRO Marine & Atmospheric Research, Aspendale, VIC, Australia*

Contact: Dr. Melody Avery, Melody.A.Avery@nasa.gov

Introduction: NASA's CALIPSO satellite carries both the Cloud and Aerosol Lidar with Orthogonal Polarization (CALIOP) and the Imaging Infrared Radiometer (IIR). The lidar is ideally suited to viewing the very top of tropical cyclones, and the IIR provides critical optical and microphysical information. The lidar and the IIR data work together to understand storm clouds since they are perfectly co-located, and big tropical cyclones provide an excellent complex target for comparing the observations. There is a lot of information from these case studies for understanding both the observations and the tropical cyclones, and we are just beginning to scratch the surface of what can be learned. Many tropical cyclone cloud particle measurements are focused on the middle and lower regions of storms, but characterization of cyclone interaction with the lowermost stratosphere at the upper storm boundary may be important for determining the total momentum and moisture transport budget, and perhaps for predicting storm intensity as well. A surprising amount of cloud ice is to be found at the very top of these big storms.

CALIOP measures 532 nm backscattered light, at both parallel and perpendicular polarizations. The backscattered signal, with 60 m vertical resolution, provides an accurate measurement of tropical cyclone cloud top heights. Ice water content is parameterized from optical extinction coefficients, using an empirical relationship derived from aircraft measurements (Heymsfield et. al., 2005). Extinction coefficients are retrieved as the 532 nm beam penetrates the cloud deck, until attenuation occurs at an effective optical depth of approximately three, with some penetration depths greater than this due to multiple scattering effects. Depolarization by cloud ice particles provides some insight about particle phase and habit. CALIOP sensitivity to cloud ice water content in the uppermost layer is 0.1 mg/m^3 (Avery et. al., 2012), a detection range that includes sub-visible cirrus and allows CALIOP to accurately measure cloud top height in the storm core and also in the associated rain bands and extended cirrus shield.

The IIR has 3 medium-resolution channels centered at 8.65 μm, 10.6 μm and 12.05 μm. The Level 1 IIR radiances are registered on a reference grid centered on the CALIOP ground track, with 1 km horizontal resolution over a 69-km swath. Effective emissivities and optical depths are retrieved for suitable scenes selected according to the vertical information provided in the CALIOP 5-km layer products (Garnier et al. 2012a). Ice crystal effective diameters are derived using a split-window technique and two effective microphysical indices defined as the 12.05-to-10.6 and. 12.05-to-08.65 ratios of the natural logarithm of the co-emissivities (Parol et al. 1991; Garnier et al. 2012b). Three crystal models have been selected in the Ping Yang data base (Yang et al. 2005) as representative of the families of relationships between both microphysical indices. The LUTs are built off-line using the FASDOM) radiative transfer model (Dubuisson et al. 2008) assuming a mono-disperse distribution. The shape index (7 for aggregates-like, 8 for plates-like, and 9 for solid columns-like) refers to the crystal model providing the best agreement between the 12.05/08.65 and the 12.05/10.6 diameters. The cloud ice water path (IWP) is estimated from a simplified expression linking optical depth and effective diameter as in Stephens (1978).

Typhoon Nida; November 28, 2009

Typhoon Nida was the most intense tropical cyclone during 2009, with a minimum central pressure of 905 hPa. Nida formed late in the season from a monsoon trough, and became a Category 5 Typhoon. The A-Train had an overpass of the storm when it was at or near maximum intensity, with sustained winds of 130 knots and central pressure of 926 hPa. The overpass was over one edge of the Typhoon eye, which was in this case covered at high altitude with cirrus clouds observed by the IIR and CALIOP. The radar observed heavy rain near the ocean surface. The Nida overpass makes an ideal case study for understanding how the instruments perform while observing deep convection. The optical depth of the storm varies, so a comparison can be made of one big convective system that has many varied conditions associated with it. The core of Nida is opaque to the lidar, but the edges of the storm are transparent. The cloud tops reach to 18 km, not only above the eyewall and core, but also at the transparent edges of the storm where they remain almost as high. CALIOP sees a very thin, wispy layer of barely visible cirrus at 19 km above the eye. The IIR shows the variation in effective particle size and optical properties. This initial comparison suggests that a much more detailed case study of Typhoon Nida will be rewarding.

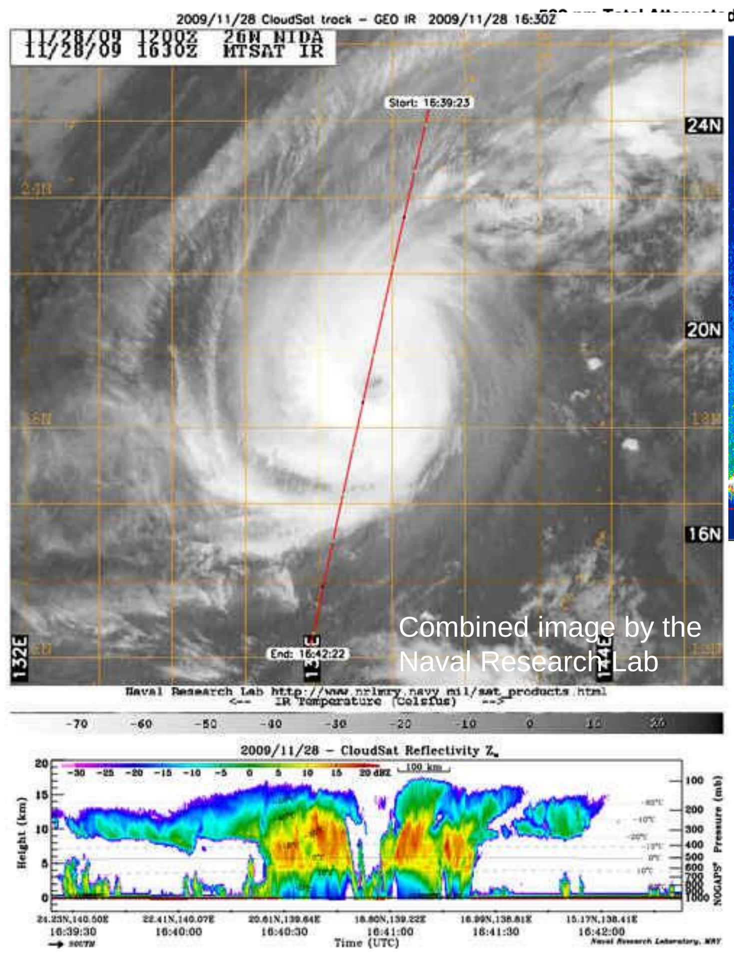

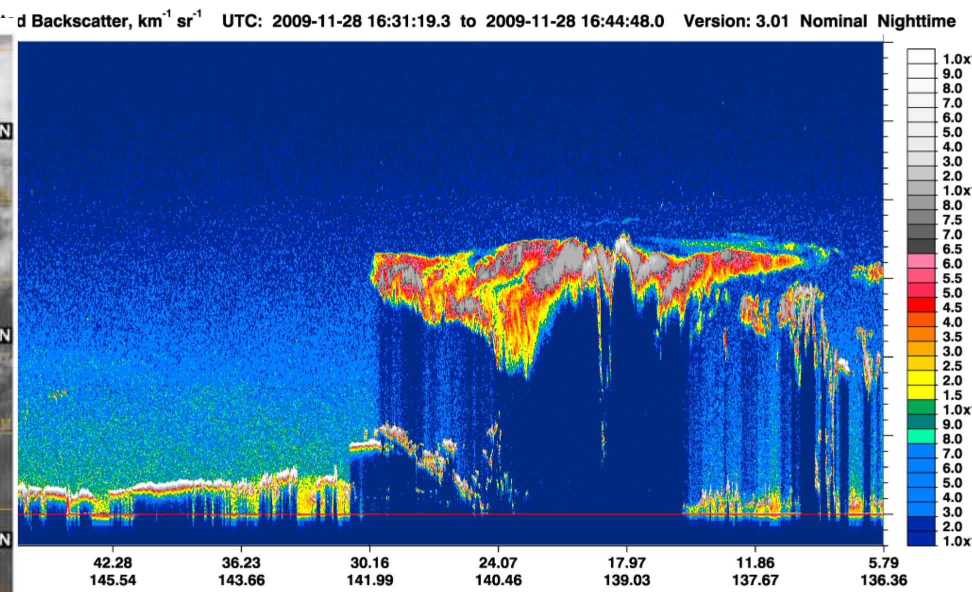

Three Views of Typhoon Nida: MODIS, CPR and CALIOP each view Typhoon Nida differently. The CloudSat CPR reflectivity and CALIOP attenuated backscatter are the most basic observations made by these active instruments. The CALIOP image clearly shows the structure in the upper-level clouds at the storm core. The CPR penetrates down into the storm core where the CALIOP laser beam has become attenuated, until it, too is attenuated by heavy rain near the surface.

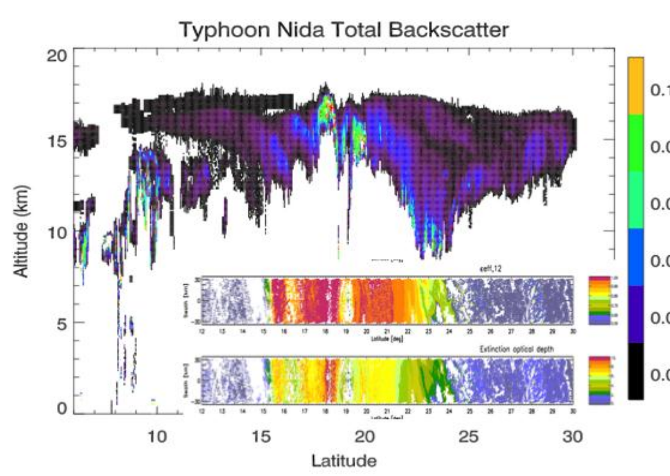

CALIOP Total Backscatter with IIR Emmisivity and Optical Depth: Since the IIR and CALIOP are perfectly co-located there is good correlation between the two instruments, as seen here.

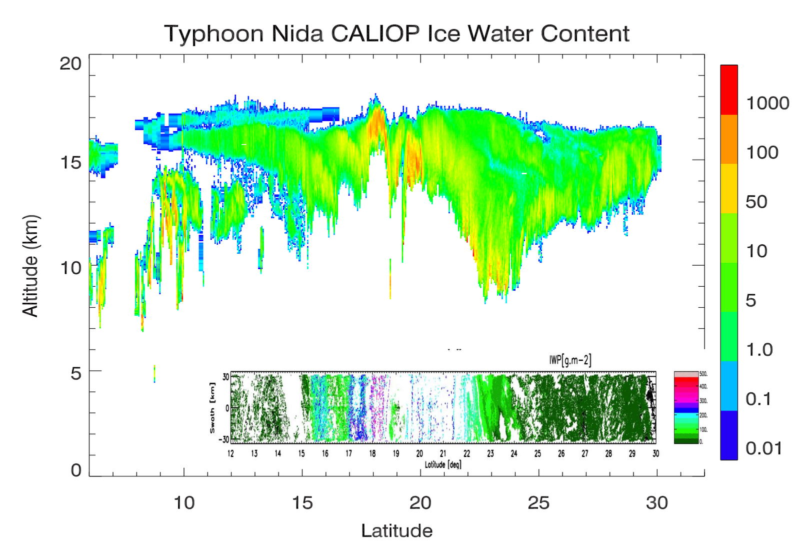

CALIOP Ice Water Content and IIR Ice Water Path

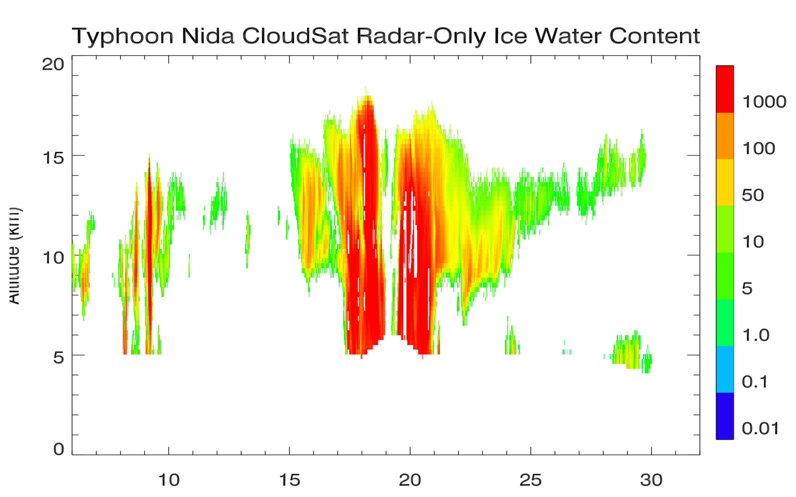

Cloud Physics Radar Ice Water Content; Radar-Only

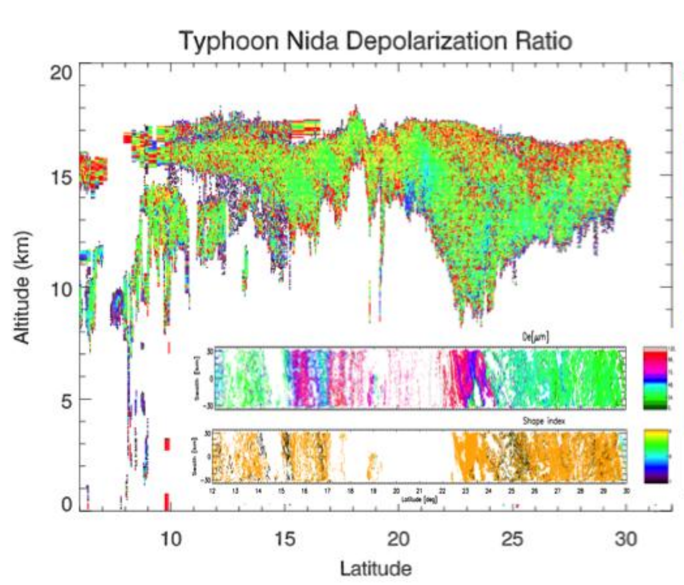

Depolarization, Effective Diameter and Shape Index: At the cloud tops, the more highly depolarizing particles appear to be smaller. These combined parameters show the changing microphysics throughout the tropical cyclone.

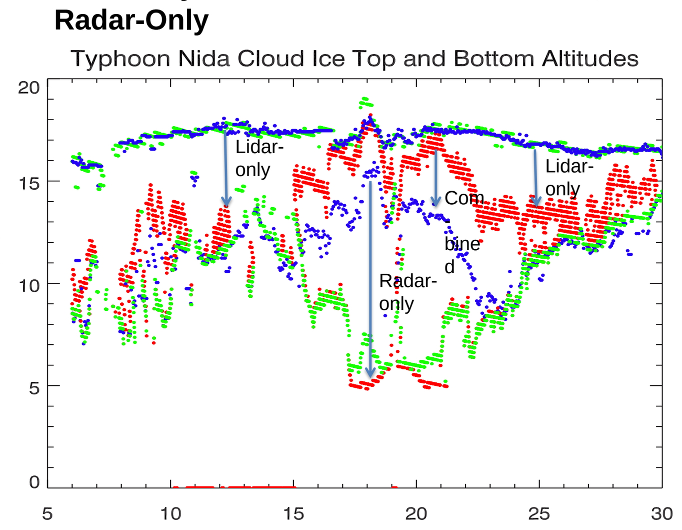

CALIOP (lidar, blue), CPR (radar, red), and 2C-ICE (combined retrieval, green) Cloud Extent

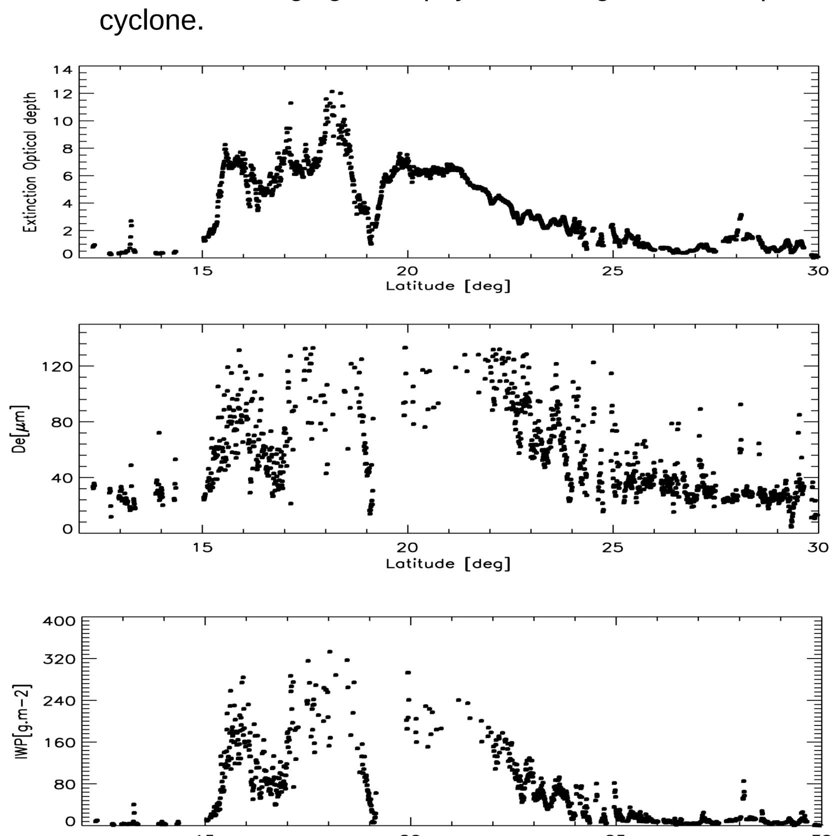

IIR Optical Depth, Effective Diameter and Ice Water Path: The IIR retrieves larger particle diameters and optical depth on the southern side of the storm, and the storm asymmetry is apparent.

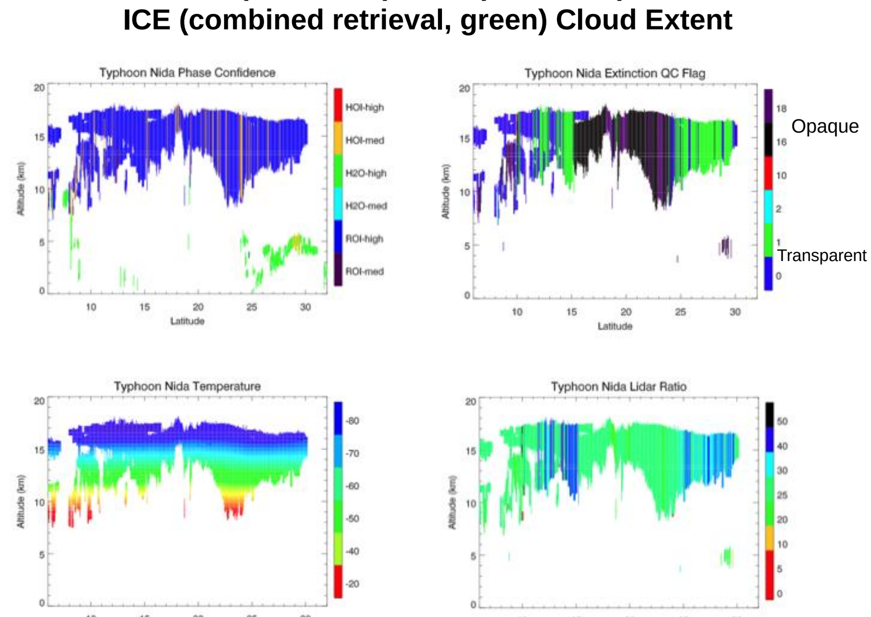

CALIOP Phase Confidence, Extinction Quality Flag, GEOS 5.2.0 Temperature and Extinction to Backscatter Ratio: The CALIOP extinction retrieval uses a range invariant extinction to backscatter (lidar) ratio (Young and Vaughan, 2009) for each 5 km horizontal analyzed segment of cloud. A constant lidar ratio may not always be true for deep convective clouds.

LITE Observes Super Typhoon Melissa

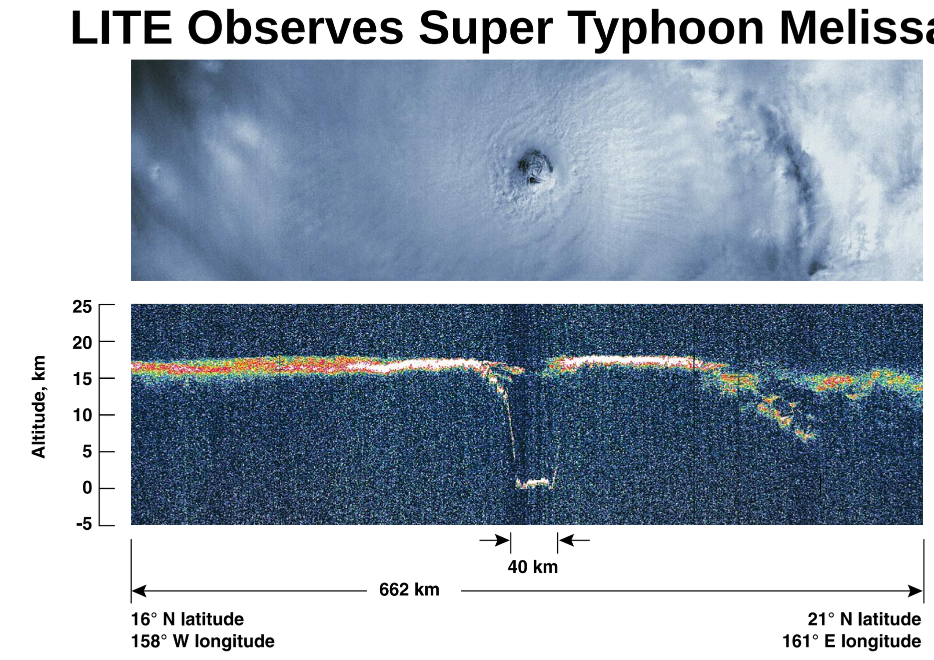

The first lidar overpass of a tropical cyclone from space. This is an overpass of Supertyphoon Melissa, on September 15,1994, with 532 nm backscatter measured by the Lidar In-space Technology Experiment on Space Shuttle Discovery. This mission was a critical precursor to the Clouds and Aerosol Lidar with Orthogonal Polarization on the CALIPSO satellite, operational in June, 2006. The overpass is described in detail in Platt et. al., 1999.

The CALIPSO CALIOP and IIR operational products (Version 3) are available at:

NASA LaRC ASDC (http://eosweb.larc.nasa.gov/) and ICARE (http://www.icare.univ-lille1.fr/)

References:

Avery et. al. (2012); *Geophys. Res. Lett*., **19**, L05808, doi:10.1029/2011GL050545.

Dubuisson et al. (2008); *J. Appl. Meteor. Climatol.*, **47**, 2545-2560.

Garnier et al. (2012a); *J. Appl. Meteorol. Clim.*, **51**, 1407-1425.

Garnier et al. (2012b); to be submitted to *J. Appl. Meteorol. Clim.*

Heymsfield, Winker and van Zadelhoff (2005) *Geophys. Res. Lett., 32*, L10807, doi:10.1029/2205GL022742.

Mace et al. (2009); *J. Geophys. Res., 114*, D00A26, doi:10.1029/2007JD009755.

Mace and Deng (2011); 2C-ICE Process Description Document

Parol et al. (1991); *J. Appl. Meteor.*, **30**, 973-984.

Platt et al. (2005); *J. Appl. Meteor.*, **38**, 1330-1345, doi:10.1175/1520-0450.

Stephens (1978); *J. Atmos. Sci.* **35**, 2123-2132.

Winker et al. (2009); *J. Atmos. Oceanic Tech.*, **26**, 2310-2323, doi:10.1175/2009JTechA1281.1.

Yang et al. (2005); *Appl. Opt.*, **44,** 5512-5523.

Young and Vaughan (2009); *J. Atmos. Oceanic Tech., 26*, 1105-1119, doi: 10.1175/2008JTechA1221.1

Hurricane Sandy; October 29, 2012

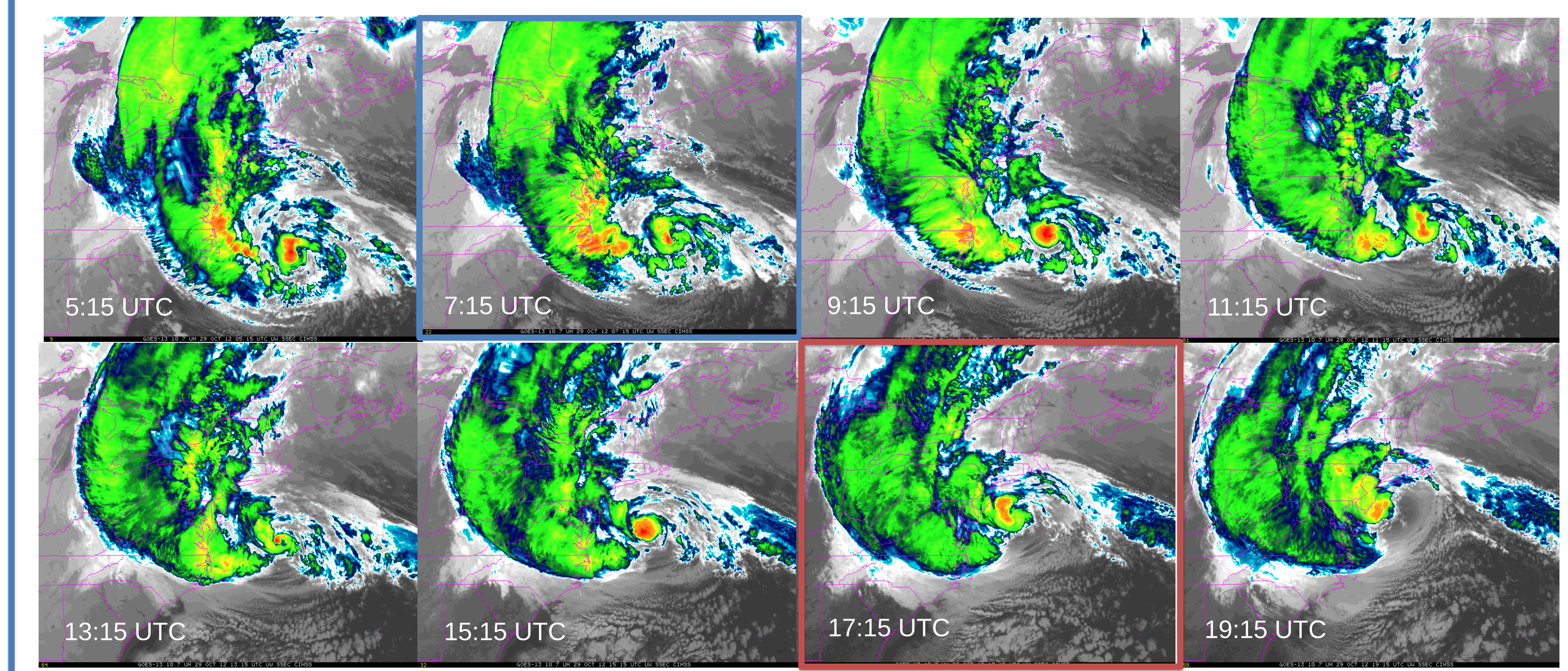

NOAA/NASA GOES-13 10.7 μm IR images from October 29, 2012, enhanced by the SSEC at the University of Wisconsin, CIMSS. The images show the storm development and merging with an extratropical system just before landfall. The CALIPSO satellite overpasses of Sandy on this day occurred at ~7:15 UTC (nighttime overpass, outlined in blue) and at ~17:15 UTC (daytime overpass, outlined in red). During the night the VIIRS instrument also captured an image of the storm, and during the day MODIS and CloudSat also provide data.

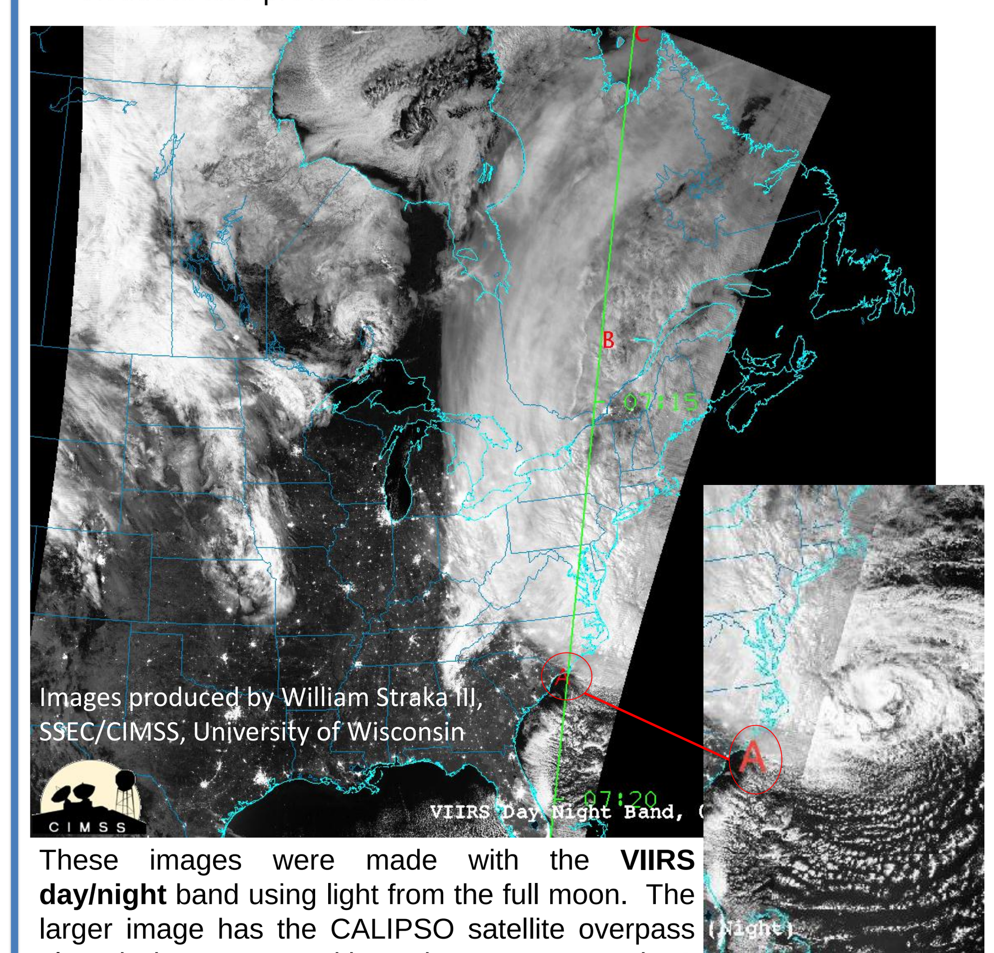

These images were made with the **VIIRS day/night** band using light from the full moon. The larger image has the CALIPSO satellite overpass plotted in green, with points A, B and C corresponding to these labeled points on the CALIOP and IIR data plots. The smaller image shows the location of Hurricane Sandy on the previous NPP overpass.

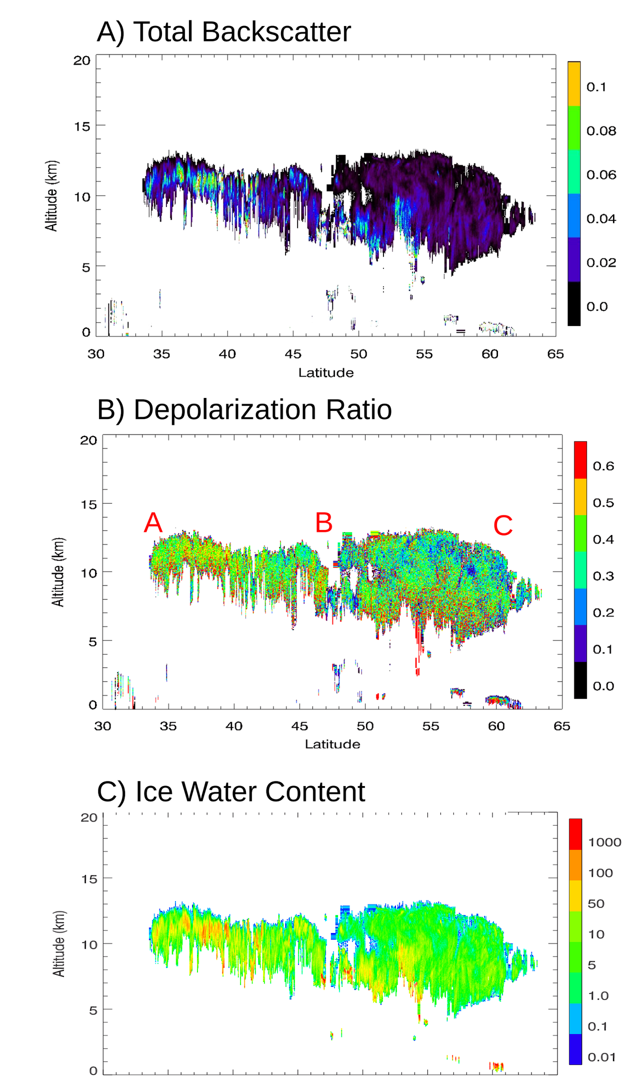

CALIOP Cross Section of Hurricane Sandy and the northern storm: The October 29 nighttime A-Train Sandy overpass provides a unique opportunity to study the difference between tropical cyclone (A-B) and extratropical Cirrus clouds (B-C). The ice particles in the tropical convective Cirrus have much higher total backscatter, ice water content and depolarization ratio than in the extratropical Ci. The lidar beam penetrates much farther into the northern clouds, maybe partially due to multiple scattering. The extratropical cloud tops are slightly higher those of Sandy.

IIR Swath Images of Hurricane Sandy

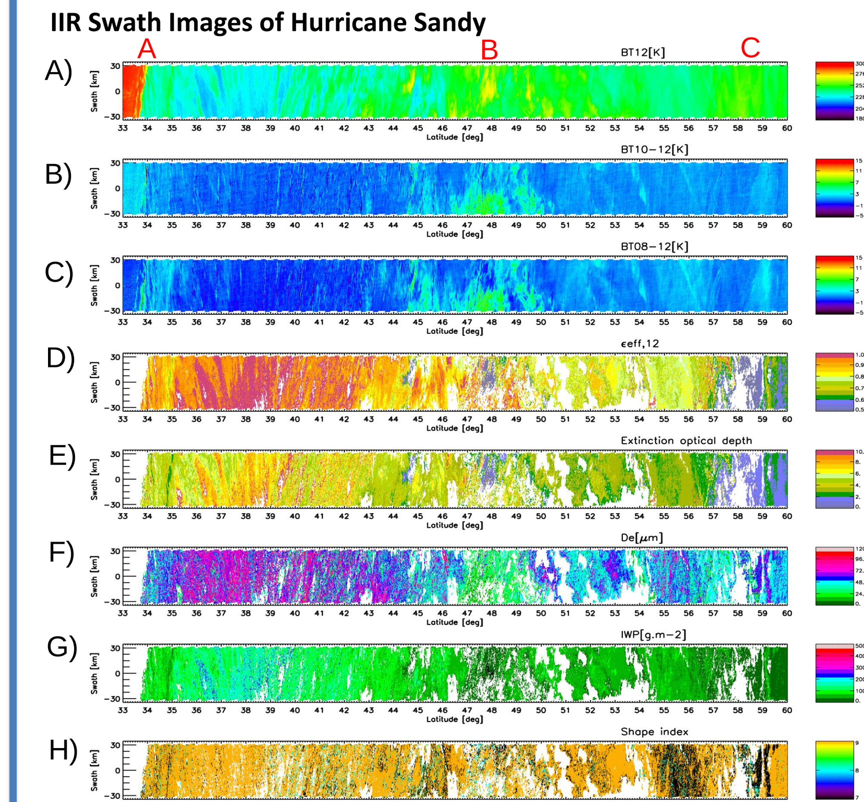

Optical and Microphysical Cloud Particle Properties derived from the IIR 8.65, 10.6 and 12.05 μm channels also show the difference between the more tropical and extratropical Cirrus associated with Sandy. The optical depth (E) and effective diameter (F) are larger in the tropical Ci, as is the ice water path (G). A shape index also varies (H: 7 for aggregates-like, 8 for plates-like, and 9 for solid columns-like).

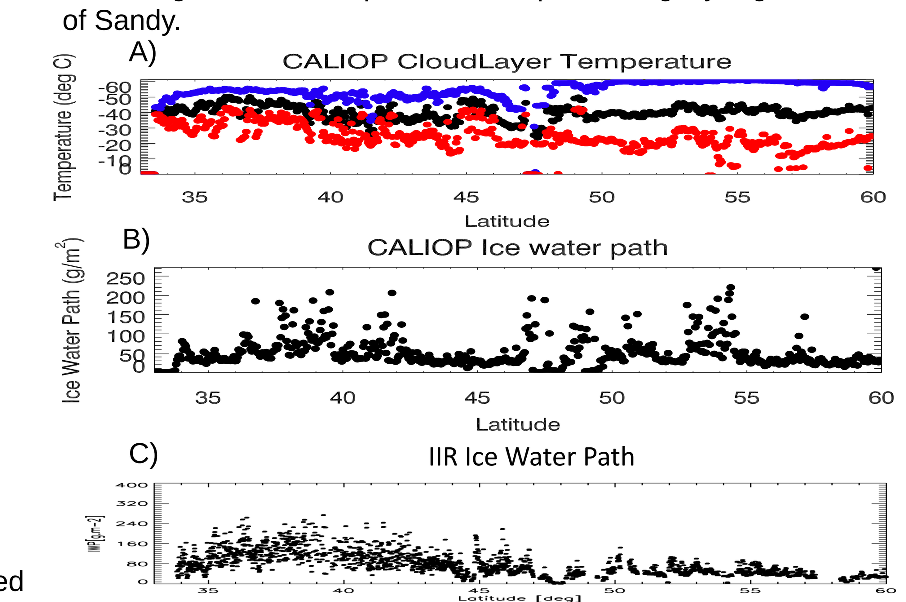

Cloud Temperature and Ice Water Path: Plot A is the cloud top, bottom and average temperature from the GMAO GEOS 5.7.2 interpolated meteorological assimilation. The range of temperatures is largest for the extratropical clouds. Plots B and C are the CALIOP and IIR derived cloud ice water paths, respectively.

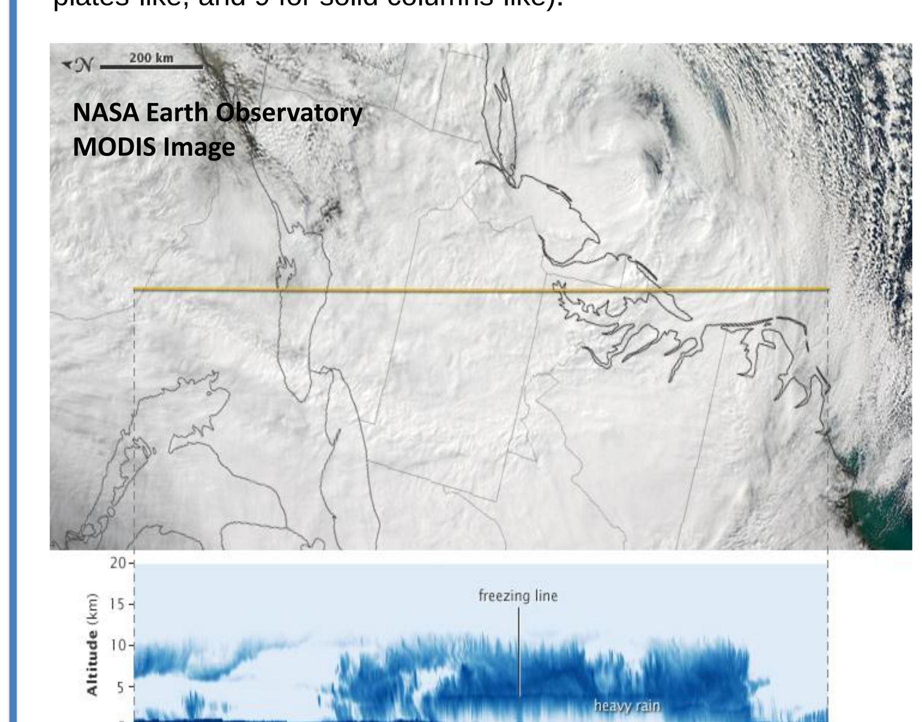

Daytime overpass of Sandy, just before landfall: The A-Train passed over the western edge of Hurricane Sandy on October 29 at ~ 17 UTC, 3 am (EDT). The images illustrate how complementary the CloudSat radar and CALIOP are in providing a rapid assessment of the Hurricane. CloudSat (left) indicates the thick lower clouds and rain, while CALIOP provides cloud top height and ice water content above 10 km.

Hurricane Sandy Ice Water Content from CALIOP